

Hereditary Lattice Corneal Dystrophy Is Associated with Corneal Amyloid Deposits Enclosing C-Terminal Fragments of Keratoepithelin

Barbara Stix,¹ Martina Leber,² Peter Bingemer,¹ Christof Gross,³ Josef Rüschoff,³ Marcus Fändrich,⁴ Daniel F. Schorderet,⁵ Christian K. Vorwerk,⁶ Martin Zacharias,⁷ Albert Roessner,¹ and Christoph Röcken¹

PURPOSE. To investigate the molecular basis of hereditary lattice corneal dystrophy (LCD) type IIIA associated with corneal amyloid deposits afflicting several members of a four-generation family.

METHODS. Histologic, immunohistochemical and biochemical studies were performed on corneal tissue samples obtained after perforating keratoplasty. DNA was extracted from peripheral blood leukocytes. All exons of the keratoepithelin-encoding *TGFBI* gene were amplified and sequenced. The presence of a mutation was confirmed by digestion of the isolated PCR product with the restriction enzyme *AlwNI*.

RESULTS. The cornea of the index patient (II-1) contained large patchy deposits of amyloid, which were immunoreactive for the C terminus of keratoepithelin. Western blot analysis of the polypeptide chains extracted from the amyloid deposits of paraffin-embedded tissue revealed that these represented mainly fragments of the full-length protein. The smallest fragments were 6.5 and 6.9 kDa. DNA analyses of the *TGFBI* gene revealed a heterozygous T→C transition at the second position of codon 540 in exon 12, indicating that replacement of phenylalanine by serine (Phe540Ser) leads to dominant disease. The mutation creates a new restriction site for the enzyme *AlwNI*. Five of the examined family members carried this mutation. Three of them (aged ≥41 years) had the disease, two family members (aged <20 years) do not yet show any clinical symptoms. An additional inconsequential single-nucleotide polymorphism (T1667C) was found at the third position of the same codon (Phe540Phe) in three unaffected family members.

CONCLUSIONS. This is the first report of a single-nucleotide mutation at codon 540 of *TGFBI* leading to LCD, and the first to demonstrate that the amyloid deposits in LCD contain proteo-

lytic fragments of keratoepithelin. (*Invest Ophthalmol Vis Sci.* 2005;46:1133–1139) DOI:10.1167/iovs.04-1319

The human transforming growth factor β -induced (*TGFBI*; OMIM 601692; Online Mendelian Inheritance in Man; <http://www.ncbi.nlm.nih.gov/Omim/>) provided in the public domain by the National Center for Biotechnology Information, Bethesda, MD) gene located on chromosome 5 at q31 encodes keratoepithelin, a 68-kDa protein that is expressed on the surface of corneal epithelial cells.¹ Mutations in the *TGFBI* gene have been linked with five distinct corneal dystrophies (CDs): granular Groenouw type 1, Reis-Bückler CD, lattice (LCD) types I and IIIA, and the Avellino CD. Most forms of CD are inherited in an autosomal dominant manner and lead to visual impairment by interfering with corneal transparency. LCD encompasses a group of diseases that is characterized by the deposition of amyloid in the cornea. LCD I is the classic form of the disease. Onset of symptoms (epithelial erosions and decreased visual function) is at the end of the first decade, with a slow progression. Substantial discomfort and visual impairment occur late in the fifth decade. A net of fine linear opacities within the corneal stroma, as a result of the accumulation of amyloid, is characteristic of LCD I. In LCD IIIA, the opacities are markedly thicker, but both LCD I and -IIIA start in the center and at the surface of the corneal stroma. In time, the opacities spread to the deeper corneal layers and to the periphery.

Studies of the molecular basis of the corneal dystrophies have revealed that LCD I and -IIIA are caused by single point mutations in exons 4, 11, 12, and 14 of the *TGFBI* gene.^{2–7,8} Herein, we describe a family that was found to have amyloid deposits within the cornea caused by a novel mutation in the *TGFBI* gene, leading to marked loss of visual acuity in the late fourth and early fifth decades of life.

MATERIALS AND METHODS

Patients

All patients studied were examined with DNA sequencing, as described later in this section. In tissue from the index patient, histologic, immunohistochemical, biochemical, and molecular biological studies were performed. Full informed consent was obtained from all family members for molecular biological analyses, in keeping with the guidelines of the Declaration of Helsinki.

Histology

Corneal tissue specimens were fixed in formalin and embedded in paraffin. Deparaffinized sections were stained with hematoxylin and eosin. The presence of amyloid was demonstrated by the appearance of green birefringence from Congo red staining under polarized light.⁹

From the ¹Institute of Pathology and the ⁶Department of Ophthalmology, Otto-von-Guericke University, Magdeburg, Germany; the ²Department of Ophthalmology and the ³Institute of Pathology, Klinikum Kassel, Kassel, Germany; the ⁴Institute of Molecular Biotechnology, Jena, Germany; the ⁵Institut de Recherche en Ophthalmologie, Sion, Switzerland; and the ⁷Department of Computational Biology, International University, Bremen, Germany.

Supported by grants from the Boehringer Ingelheim Foundation, Heidesheim, Germany. MF is supported by a BioFuture grant.

Submitted for publication November 10, 2004; revised December 22, 2004; accepted January 3, 2005.

Disclosure: **B. Stix**, None; **M. Leber**, None; **P. Bingemer**, None; **C. Gross**, None; **J. Rüschoff**, None; **M. Fändrich**, None; **D.F. Schorderet**, None; **C.K. Vorwerk**, None; **M. Zacharias**, None; **A. Roessner**, None; **C. Röcken**, None

The publication costs of this article were defrayed in part by page charge payment. This article must therefore be marked "advertisement" in accordance with 18 U.S.C. §1734 solely to indicate this fact.

Corresponding author: Christoph Röcken, Institute of Pathology, Otto-von-Guericke-University, Leipziger Strasse 44, D-39120 Magdeburg, Germany; christoph.roecken@medizin.uni-magdeburg.de.

Immunohistochemistry

Immunostaining was performed with monoclonal antibodies directed against AA amyloid (1:400; Dako, Hamburg, Germany), and gelsolin (1:1000; Sigma-Aldrich, Deisenhofen, Germany) and with polyclonal antibodies directed against the amyloid P-component (1:1600), fibrinogen (1:1000), lactoferrin (1:800), lysozyme (1:3000), transthyretin (1:600), λ -light chain (1:10,000), κ -light chain (1:10,000; all Dako), apolipoprotein AI (ApoAI; 1:1500), and keratoepithelin (KE2 and KE15). The antibodies directed against keratoepithelin had been raised in rabbits by using the C (amino acids 426-682)- and N (amino acids 69-364)-terminal portions of keratoepithelin, as described elsewhere.¹⁰ Before they were immunostained, the specimens were treated with 10 mM EDTA (two times for 10 minutes each, 450-W microwave oven; amyloid P component, gelsolin, and transthyretin). Immunoreactions were visualized with the avidin biotin complex method, with the use of an ABC alkaline phosphatase kit (Vectastain; Biogene-Alexis GmbH, Grünberg, Germany) or a diaminobenzidine (DAB) Detection kit (iVIEW; Ventana, Illkirch, France). Neufuchsin and 3,3'-diaminobenzidine-tetrahydrochloride, respectively, served as chromogens. The specimens were counterstained with hematoxylin. The specificity of immunostaining was verified with specimens containing known classes of amyloid (AA amyloid, ApoAI, transthyretin, λ -light chain), by using positive controls recommended by the manufacturers (remaining antibodies) and by omitting the primary antibodies.

Immunostaining with anti-KE2 and anti-KE15 antibodies was performed as described previously¹⁰ with some modifications. Briefly, after digestion with 1 U Pronase (15 minutes at room temperature; Sigma-Aldrich), the sections were blocked with normal goat serum (1:30 in TBS with 2% skimmed milk; Dako) for 10 minutes at room temperature. The primary antibodies KE2 and KE15 were both diluted 1:10 in RPMI supplemented with 5% BSA and incubated for 30 minutes at room temperature. The immunoreaction was visualized with the avidin biotin complex method (Vectastain ABC kit; Biogene-Alexis GmbH). Fast red served as the chromogen.

SDS-PAGE and Western Blot Analysis

Amyloid fibril proteins were extracted from formalin-fixed and paraffin-embedded specimens and resolved by SDS polyacrylamide gel electrophoresis, as described elsewhere, using specimens from the index patient (II-1).¹¹ As negative controls, we used amyloid fibril proteins, extracted with the same methodology from formalin-fixed amyloid-laden tissue specimens, obtained from a patient with immunoglobulin-associated AL amyloidosis and from a patient with secondary AA amyloidosis. Proteins were visualized by Coomassie blue staining or blotted onto polyvinylidene difluoride (PVDF) membranes. Immunostaining of the transferred proteins was performed with anti-KE2 (dilution 1:2000) and anti-KE15 (1:100) as primary antibodies (room temperature, 1 hour). Blocking was performed in Tris-buffered saline containing 3% bovine serum albumin and 0.05% Tween-20. The membranes were then incubated for 1 hour with the secondary antibody (1:2000 dilution of goat anti-rabbit-AP). The substrate (BCIP/NBT (Pierce, Rockford, IL) was left on the membrane until distinct bands had developed.

Isolation and Amplification of Genomic DNA

Genomic DNA was extracted from peripheral blood leukocytes with a kit (NucleoSpin Blood L Kit; Macherey & Nagel, Düren, Germany). Exons 1 to 17 of the *TGFBI* gene were amplified by PCR with 1 μ g of genomic DNA of individual II-1, and the primers are listed in Table 1. Initial denaturation and activation of *Taq* polymerase at 95°C for 5 minutes was followed by 35 cycles (30 for exons 4 and 11) with denaturation (95°C, 30 seconds), annealing for 30 seconds (temperatures listed in Table 1), an extension at 72°C for 60 seconds, and a final extension at 72°C for 15 minutes. The coding region for the classic mutation Asp187 of the gelsolin gene was amplified with the following

TABLE 1. Primer Sequences and Annealing Temperatures for Keratoepithelin

Exon	Primer Sequences	T _a
1	5'-TC TCA CTT CCC TGG AG-3'	56
	5'-GAC TAC CTG ACC TTC CGC AG-3'	56
2	5'-GGT GGA GGT GCT GAT CAT CT-3'	56
	5'-AGC CAG CGT GCA TAC AGC TT-3'	56
3	5'-TTC ACC CAC CAT TCC TCT TC-3'	56
	5'-GGT ACT CCT CTC TCC CAC CA-3'	56
4*	5'-ATC CCT CCT TCT GCT TTC TG-3'	59
	5'-GCA GAC GGA GGT CAT CTC AC-3'	59
5	5'-TTA AAC ACA GAG TCT GCA GC-3'	56
	5'-TTC ATT ATG CAC CAA GGG CCA-3'	56
6	5'-TGT TGA CTG CTC ATC CTT GC-3'	53
	5'-CTC TTG GGA GGC AAT GTG TC-3'	53
7	5'-CTT CAG GGA GCA CTC CAT C-3'	57
	5'-AAT CTA GCT GCA CCA ATG AGG-3'	57
8	5'-CTT GAC CTG AGT CTG TTT GGA-3'	56
	5'-GGA TGG CAG AAG AGA TGG TG-3'	56
9	5'-CCT GCT GAT GTG TGT CAT GC-3'	57
	5'-CTG CCT CCA GGC ACA ATC TA-3'	57
10	5'-TCA TTG CAG GAG CAC ATC TC-3'	57
	5'-CCC AGG AGC ATG ATT TAG GA-3'	57
11*	5'-GAG GCC CCT CGT GGA AGT A-3'	57
	5'-ACA TCC CAC TCC AGC ATG AC-3'	57
12	5'-CTG TTG ACA GGT GAC ATT TTC-3'	60
	5'-ATG TGC CAA CTG TTT GCT GCT-3'	60
13	5'-GGG ATT AAC TCT ATC TCC TT-3'	56
	5'-TGT GTA TAA TTC CAT CCT GA-3'	56
14	5'-TCA GTA AAC ACT TGC TGA GTG AA-3'	61
	5'-ACT GCC ACA TGG AGA AAA GGA C-3'	61
15	5'-CCT CAG TCA CGG TTG TTA TG-3'	56
	5'-CTC TAT GGC CCA AAC AGA GG-3'	56
16	5'-TTG TCA TAA GCA GTT GCA GG-3'	56
	5'-GCT TGC TTG GGG GTA AGG-3'	56
17	5'-TCC TAG ACA GAC ATG GGG AGA-3'	60
	5'-TGA GAG AAA TTG GCG GAG AG-3'	60

T_a, annealing temperature °C.

* Number of cycles: 30

primers: 5'-ACT GGT CTA CTG TGT CTC TA-3' and 5'-TCT TCA GCC CAC ACT TTC TG-3'. The PCR profile for gelsolin was as follows: 94°C, 3 minutes; 35 cycles (94°C, 1 minute; 55°C, 1 minute; 72°C, 1 minute); and an extension of 72°C, 10 minutes. The PCR products were isolated (NucleoSpin Extract; Macherey & Nagel) and sequenced with dye-termination chemistry (Prism Big Dye Terminator ver.1.1, Ready Reaction kit; Applied Biosystems, Inc. [ABI], Darmstadt, Germany) with a capillary sequencer (Prism model 310; ABI).

Restriction Enzyme Digestion with *AlwNI*

Restriction-enzyme digestion analysis was performed to confirm the mutation found. This mutation creates a new restriction site for *AlwNI* (CAGNNN/CTG). One microgram of the purified DNA fragment obtained by the PCR with the primer for exon 12 (Table 1) was incubated with 5 U *AlwNI* at 37°C for 2 hours. The digestion was stopped by heat inactivation (65°C, 30 minutes) according to the manufacturer's instructions. The samples were separated on a 9% polyacrylamide gel and visualized with a silver staining procedure.

Homology Modeling

The model was generated using MODELLER,¹² based on a sequence alignment of keratoepithelin domain 4 (Swiss Prot: Q15582, residues 502-635; <http://www.expasy.org>; provided in the public domain by the Swiss Institute of Bioinformatics, Geneva, Switzerland) to the known *Drosophila melanogaster* fasciclin I domain four-template structure¹³ according to a procedure by Clout and Hohenester.¹⁴

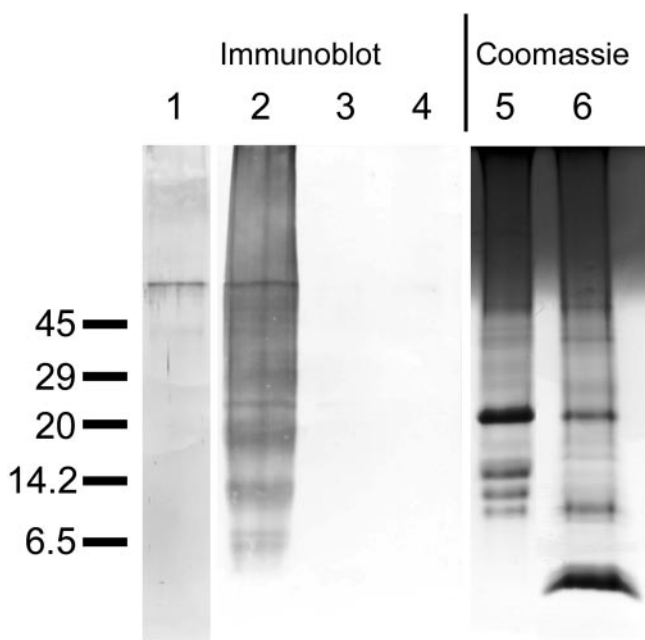


FIGURE 4. Amyloid proteins were extracted from formalin-fixed specimens obtained from the cornea of the index patient (II-1). After SDS-PAGE and Western blot analysis with anti-KE15 (lane 1) and anti-KE2 (lane 2) antibody, a distinct band was found at 68 kDa that was compatible with intact keratoepithelin. Further bands were found after blot analysis with anti-KE2 (lane 2), probably representing the amyloid proteins. The anti-KE2 antibody did not stain amyloid proteins extracted from formalin-fixed tissue specimens containing AL (lane 3) or AA (lane 4) amyloid. Coomassie staining revealed the banding pattern of AL (lane 5) and AA (lane 6) amyloid proteins.

antibodies intensely stained the surface epithelium—the location of native keratoepithelin (Fig. 3)—and immunostaining was abolished after omission of the primary antibody (Fig. 3).

SDS-PAGE and Western Blot Analysis

Amyloid fibril proteins were extracted from formalin-fixed and paraffin-embedded biopsy specimens of the cornea, which were shown histologically to enclose amyloid deposits, and were resolved by denaturing gel electrophoresis. The amount of amyloid proteins extracted was low and could not be visualized by Coomassie blue or silver staining (data not shown). However, using Western blot analysis with the antibodies KE15 and KE2, we were able to detect a protein band at 68 kDa, which represents mature, full-length keratoepithelin (Fig. 4). In addition, the amyloid-specific antibody KE2 detected a range of further bands, which shows that keratoepithelin or fragments of the full-length protein are smeared across most of the lane, a property that is commonly encountered when trying to separate tissue-purified amyloids on an SDS-gel. This effect is caused most likely by cross-linking of the amyloid proteins after formalin fixation, as this smear was not observed after immunoblot analysis with the antibody directed against the N-terminal portion of keratoepithelin. In addition, KE2 but not KE15 detects in the low molecular range several distinct bands corresponding to masses of 6.5, 6.9, 14, 17, and 21 kDa, representing peptide fragments arising from the C terminus of keratoepithelin (Fig. 4). These data demonstrate that amyloid deposits derived from keratoepithelin do not contain mainly the full-length protein, but rather fragments thereof. Native, unfixed corneal tissue was not available from any of the family members. The specificity of immunoblot analysis was further

tested by using AL and AA amyloid proteins extracted from formalin-fixed tissue obtained from a patient with primary AL amyloidosis (Fig. 4, lane 5)¹⁵ and from a patient with chronic rheumatoid arthritis (Fig. 4, lane 6). Several amyloid proteins were found after Coomassie blue staining, some of which had been identified by amino acid sequencing.¹⁵ Similar to corneal amyloid (Fig. 4, lane 2), a protein smear related to cross-linking of the amyloid proteins after formalin fixation was found (Fig. 4, lanes 5, 6). However, neither the AL nor the AA amyloid proteins immunoreacted with the two antibodies directed against keratoepithelin (Fig. 4, lanes 3, 4).

DNA Analyses

Analysis of the exons 1 through 17 of the keratoepithelin encoding *TGFBI* gene of patient II-1 revealed a point mutation in exon 12. A heterozygous T→C transition at the second position of codon 540 was found by double-strand sequencing, leading to the replacement of the normal phenylalanine by a serine residue (Phe540Ser; Fig. 5). It is of note that this mutation occurs within the same part of keratoepithelin that was found by our antibody. Moreover, the same mutation was found in the index patient's daughter (III-1), the patient's brother (II-2), the patient's niece (III-4), and one granddaughter (IV-1; Fig. 1).

Another base change, a T→C transition at the *third* position of the same codon 540 was found in individuals II-3, III-2, III-3, and III-4, but has no effect on the amino acid encoded (Phe540Phe). This single nucleotide polymorphism is a well-documented base change in this exon.¹⁶ The sequence of individual III-4 revealed the Phe540Phe polymorphism in conjunction with the Phe540Ser mutation.

The mutation at the second position of codon 540 introduces a restriction site for the endonuclease *Alu*NI. The wild-type sequence of exon 12 (ACA GTC TTT GCT, codon 538-541) changes into ACA GTC T↓CT GCT, containing the recognition sequence for *Alu*NI (CAG NNN↓CTG). Accordingly, three distinct bands were found after the incubation of the DNA with *Alu*NI in all affected family members investigated: the full-length fragment of exon 12 of the nonmutated allele, and two shorter fragments yielded by the digestion of the mutated allele (Fig. 6). Proband II-3 served as a negative control and showed a single band only (Fig. 6, lane 3).

No mutations were found in the gelsolin gene, which is known to cause hereditary LCD II.^{17,18}

DISCUSSION

We describe here for the first time a family with hereditary LCD associated with corneal AKer amyloid deposits caused by a

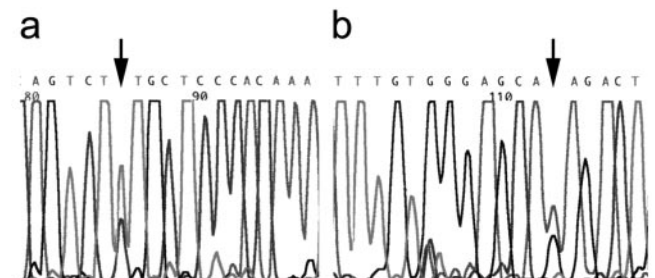


FIGURE 5. Nucleotide sequence from exon 12 of the *TGFBI* gene of the index patient II-1. The heterozygous T→C transition at position 1666 (codon 540, arrows) was confirmed by both sense (a) and antisense (b) primers. The transition of T to C results in the replacement of phenylalanine by serine.

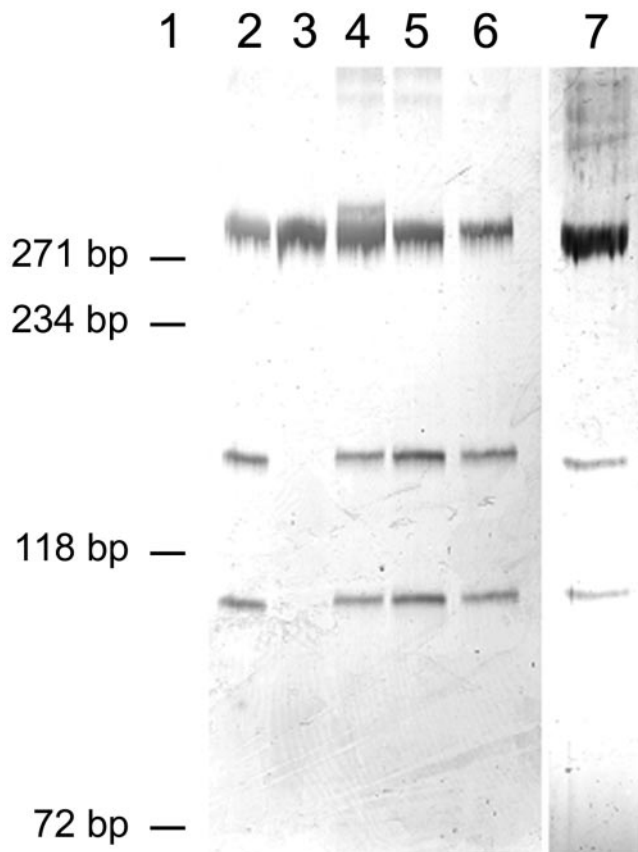


FIGURE 6. *AluNI* restriction digest. The isolated PCR products corresponding to the sequence of exon 12 of the *TGFBI* gene from patients II-1 (lane 2), III-4 (lane 4), II-2 (lane 5), III-1 (lane 6), and IV-1 (lane 7) were each incubated with 1 U of the enzyme (*AluNI*) for 2 hours at 37°C. The sample of an unaffected proband (II-3; lane 3) served as a negative control. Lane 1: base-pair standard.

dominant single-point mutation at the second position of codon 540 in exon 12 of the *TGFBI* gene, replacing phenylalanine by serine (Phe540Ser) in the adhesion molecule keratoepithelin.

AKer amyloid causes six different LCDs (LCD I, -IA, -IIIA, -IV, -VI, and -VII),¹⁴ all of which are related to point mutations in the *TGFBI* gene. These mutations, including our novel mutation T1666C, are located in the exons 4, 11, 12, or 14.¹⁴ We believe that our family has hereditary LCD IIIA. This form of corneal dystrophy was first described by Stock et al.¹⁹ in an Italian family. LCD IIIA is characterized by thick, ropy lattice lines throughout the stroma that are easily detected with direct illumination (see also Fig. 2).⁷ Histology reveals accumulation of amyloid deposits varying in size and ribbons of amyloid between the stroma and Bowman's layer.^{7,19,20} Similar to our family, the age of onset in LCD IIIA ranges from the fourth to fifth decade of life. Dighiero et al.²⁰ reported on a French family with clinically and histologically diagnosed LCD IIIA. A single base pair transition at the first nucleotide position of the codon 546 (GCC/ACC) led to the replacement of alanine by threonine (Ala546Thr) and was found in all affected individuals. Dighiero et al.²⁰ suggested that this mutation is responsible for LCD IIIA in their French family.

In addition to the Phe540Ser mutation, we found another heterozygous single-nucleotide substitution at the third position of the same codon. This T→C transition is an inconsequential single-nucleotide polymorphism, because this base

change did not alter the encoded amino acid, it did not segregate with the affected individuals in our family, and it has been reported in several studies.²¹⁻²³ The sequence of proband III-4 revealed both transitions in codon 540 (Phe540Ser and Phe540Phe), but the restriction digest resulted in the same three distinct bands observed in the other affected family members. That the inconsequential SNP would eliminate the restriction site required by the enzyme leads to the conjecture that, since the Phe540Phe polymorphism comes from the unaffected parent, the mutations must be localized on opposing alleles.

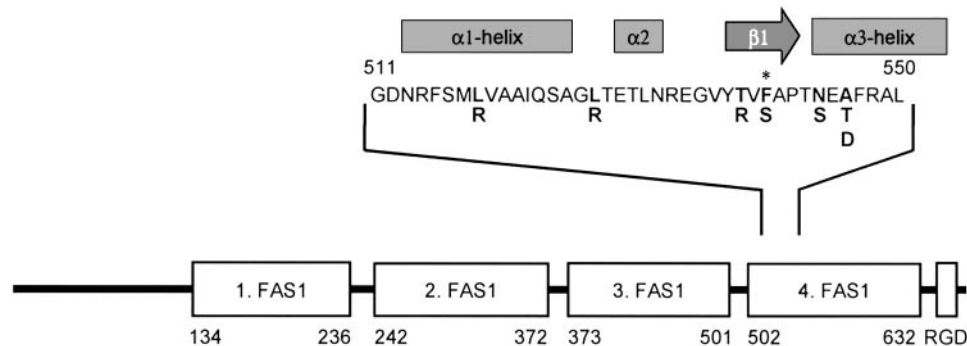
Keratoepithelin contains four FAS1 regions of internal homology of approximately 140 amino acids. All but one (Arg124Cys) mutation of the *TGFBI* gene leading to corneal dystrophy are located in the fourth FAS1 region. For exon 12, which translates into a part of this region, there are eight different mutations currently described (see Table 2).²⁴ The localization of the affected amino acids within the fourth FAS1 region seem to be the common molecular basis for the occurrence of LCDs, as there is no other correlation between the phenotypes observed.

Generally, there are two major ways by which a mutation can affect amyloid formation and aggregation, (1) by acting on the unfolded polypeptide chain and intrinsically promoting its association or (2) by destabilizing the native, globular conformation, thereby increasing the proportion of unfolded and aggregation-competent polypeptide chains. The former effect can be predicted from the rate of aggregation v_{mut} and the ratio $\ln(v_{mut}/v_{wt})$.²⁷ Using this correlation, the Phe540Ser mutation leads to a slightly negative value of $\ln(v_{mut}/v_{wt})$ (-0.19) and a decelerating effect on the aggregation kinetics. Therefore, this property does not explain its amyloid-promoting effect of mutation. By contrast, there is considerable evidence that the second type of mutagenic effect applies here—namely, the destabilization of the native, globular state which makes the polypeptide main chain more competent to form intermolecular arrangements. This evidence comes from a homology model of the fourth FAS1 region of keratoepithelin¹⁴ that has been derived from the crystal structure of its close homologue, the *Drosophila* protein fasciclin 1 (Fig. 7).¹³ This model shows that the respective region forms a compact globular structure consisting of an α -helical and a β -domain and that residue Phe540 is positioned within a β -strand. This strand runs through the center of the hydrophobic core of the β -domain (Fig. 7b). Considering the large size of phenylalanine and its ability to make very many hydrophobic contacts, replacement of such a buried residue by the much smaller side chain of polar serine readily suggests that the thermodynamic stability of the entire protein will be decreased dramatically. For comparison, when the fully buried Phe153 of the T4 lysozyme is replaced by the small hydrophobic residue Ala, it decreases the thermodynamic stability of the protein by -3.5 kcal/mol,²⁸ a value that is well within the range of values known to promote aggregation and amyloid formation.²⁹ Indeed, amyloid structures are known to form by association of at least partly, if not entirely, unfolded polypeptide chains; and stable, globular proteins must be sufficiently unfolded to enable the polypeptide backbone to form intermolecular interactions.³⁰ Moreover, unfolding also favors a proteolytic cleavage reaction.

Morand et al.³¹ demonstrated that the secretion of the recombinant proteins carrying the most common mutations (Arg124Cys and Arg555Trp) was unaffected in transfected HeLa and HCE cells, with the mutated proteins accumulating in the medium. They also showed that the accumulation of these proteins correlated with an increased apoptotic response of the affected cells. Whether the cornea lacks a general clearing mechanism in response to apoptosis, allowing for the progres-

TABLE 2. Domains of Keratoepithelin and Localization of Mutations in the Secondary Structure of Exon 12 of the *TGFBI* Gene Associated with Corneal AKer Amyloidosis

Localization of the mutation found in our kindred. α -Helices: light grey; β -strands: dark grey.



Corneal Phenotype	Mutation in <i>TGFBI</i> Gene	Reference
LCD I	Ala546Asp+Pro551Gln	Aldave et al. ² , Klintworth et al. ⁵
LCD I/IIIA	Leu518Arg	Yamamoto et al. (ARVO Abstract 563, 1999)
	Thr538Arg	Munier et al. ²⁴
	Asn544Ser	Clout and Hohenester ¹⁴
LCD intermediate	Δ Phe540	Rozzo et al. ²⁵
LCD IIIA	Phe540Ser	Present study
LCD IIIA/V	Ala546Thr	Dighiero et al. ²⁰
PCA	Ala546Asp	Eifrig et al. ¹⁶
LCD deep/IV	Leu527Arg	Fujiki et al. ²⁶

PCA, polymorphic corneal amyloidosis.

sive accumulation and deposition of mutated keratoepithelin extracellularly, as suggested by Morand et al.,³¹ or the deposition of amyloid results from the secretion of the mutated proteins, remains unclear. As mutant forms of keratoepithelin do not form amyloid deposits in the skin of patients with CD,²³ there seem to be specific components within the cornea that promote the accumulation of mutated keratoepithelin to form amyloid deposits. In this regard it was interesting to note that immunoblot analysis with site-specific antibodies detected proteolytic fragments derived from the C-terminal region of kera-

toepithelin in our index patient. After our amyloid protein extraction procedure, we also found mature keratoepithelin, which may originate from the surface epithelium. However, N-terminal cleavage products were not detected by immunoblot analysis. Further studies are needed to demonstrate whether proteolysis is a prerequisite and essential for the formation of amyloid, as in Alzheimer's disease, or whether it occurs after amyloid has been formed and represents a frustrated attempt to clear pathologic corneal protein aggregates.³² This ultimately may improve our understanding of the pathologic course and pathogenesis of CDs and lead to the development of new treatment strategies, other than perforating keratoplasty.

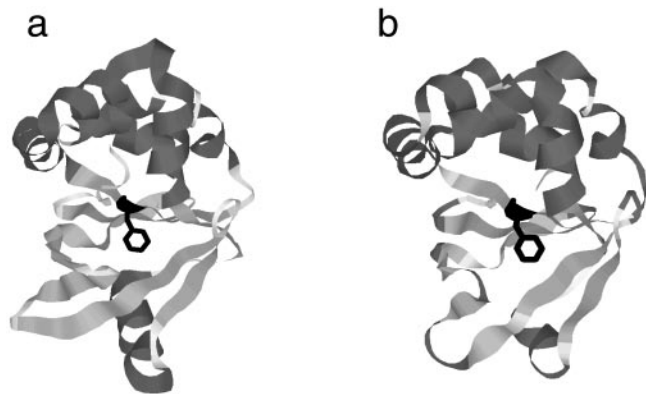


FIGURE 7. Ribbon representations of fasciclin-1 (a) and the homology model of keratoepithelin (b) fourth FAS1 domain, illustrating their compact and globular structure. Residue Phe540 (b) is shown in black. It is located within a β -strand that runs through the center of the hydrophobic core. Dark gray: α -Helices; light gray: β -strands. The figure was generated with the program Rasmol ver. 2.6 (<http://openrasmol.org/>) developed by Roger Sayle and distributed as an open-source program by Bernstein & Sons Information Systems Consultants, Bellport, NY).

References

- Escribano J, Hernando N, Ghosh S, Crabb J, Coca-Prados M. cDNA from human ocular ciliary epithelium homologous to beta ig-h3 is preferentially expressed as an extracellular protein in the corneal epithelium. *J Cell Physiol.* 1994;160:511-521.
- Aldave AJ, Gutmark JG, Yellore VS, et al. Lattice corneal dystrophy associated with the Ala546Asp and Pro551Gln missense changes in the *TGFBI* gene. *Am J Ophthalmol.* 2004;138:772-781.
- Munier FL, Korvatska E, Djemai A, et al. Kerato-epithelin mutations in four 5q31-linked corneal dystrophies. *Nat Genet.* 1997;15:247-251.
- Klintworth GK. Advances in the molecular genetics of corneal dystrophies. *Am J Ophthalmol.* 1999;128:747-754.
- Klintworth GK, Bao W, Afshari NA. Two mutations in the *TGFBI* (*BIGH3*) gene associated with lattice corneal dystrophy in an extensively studied family. *Invest Ophthalmol Vis Sci.* 2004;45:1382-1388.
- Yamamoto S, Okada M, Tsujikawa M, et al. The spectrum of beta ig-h3 gene mutations in Japanese patients with corneal dystrophy. *Cornea.* 2000;19:S21-S23.

7. Yamamoto S, Okada M, Tsujikawa M, et al. A kerato-epithelin (betaig-h3) mutation in lattice corneal dystrophy type IIIA. *Am J Hum Genet.* 1998;62:719-722.
8. Stewart H, Black GC, Donnai D, et al. A mutation within exon 14 of the TGFBI (BIGH3) gene on chromosome 5q31 causes an asymmetric, late-onset form of lattice corneal dystrophy. *Ophthalmology.* 1999;106:964-970.
9. Puchtler H, Sweat F, Levine M. On the binding of Congo red by amyloid. *J Histochem Cytochem.* 1962;10:355-364.
10. Korvatska E, Munier FL, Chaubert P, et al. On the role of keratoepithelin in the pathogenesis of 5q31-linked corneal dystrophies. *Invest Ophthalmol Vis Sci.* 1999;40:2213-2219.
11. Röcken C, Hegenbarth V, Schmitz M, et al. Plasmacytoma of the tonsil with AL amyloidosis: evidence of post-fibrillogenic proteolysis of the fibril protein. *Virchows Arch.* 2000;436:336-344.
12. Sali A, Blundell TL. Comparative protein modelling by satisfaction of spatial restraints. *J Mol Biol.* 1993;234:779-815.
13. Clout NJ, Tisi D, Hohenester E. Novel fold revealed by the structure of a FAS1 domain pair from the insect cell adhesion molecule fasciclin I. *Structure (Camb).* 2003;11:197-203.
14. Clout NJ, Hohenester E. A model of FAS1 domain 4 of the corneal protein beta(ig)-h3 gives a clearer view on corneal dystrophies. *Mol Vis.* 2003;9:440-448.
15. Bohne S, Sletten K, Menard R, et al. Cleavage of AL amyloid proteins and AL amyloid deposits by cathepsins B, K, and L. *J Pathol.* 2004;203:528-537.
16. Eifrig DE Jr, Afshari NA, Buchanan HW, Bowling BL, Klintworth GK. Polymorphic corneal amyloidosis: a disorder due to a novel mutation in the transforming growth factor beta-induced (BIGH3) gene. *Ophthalmology.* 2004;111:1108-1114.
17. Haltia M, Prelli F, Ghiso J, et al. Amyloid protein in familial amyloidosis (Finnish type) is homologous to gelsolin, an actin-binding protein. *Biochem Biophys Res Commun.* 1990;167:927-932.
18. Maury CP, Alli K, Baumann M. Finnish hereditary amyloidosis: amino acid sequence homology between the amyloid fibril protein and human plasma gelsoline. *FEBS Lett.* 1990;260:85-87.
19. Stock EL, Feder RS, O'Grady RB, Sugar J, Roth SI. Lattice corneal dystrophy type IIIA: clinical and histopathologic correlations. *Arch Ophthalmol.* 1991;109:354-358.
20. Dighiero P, Drunat S, Ellies P, et al. A new mutation (A546T) of the betaig-h3 gene responsible for a French lattice corneal dystrophy type IIIA. *Am J Ophthalmol.* 2000;129:248-251.
21. Kim HS, Yoon SK, Cho BJ, Kim EK, Joo CK. BIGH3 gene mutations and rapid detection in Korean patients with corneal dystrophy. *Cornea.* 2001;20:844-849.
22. Schmitt-Bernard CF, Guittard C, et al. BIGH3 exon 14 mutations lead to intermediate type I/IIIA of lattice corneal dystrophies. *Invest Ophthalmol Vis Sci.* 2000;41:1302-1308.
23. Schmitt-Bernard CF, Schneider C, Argiles A. Clinical, histopathologic, and ultrastructural characteristics of BIGH3(TGFBI) amyloid corneal dystrophies are supportive of the existence of a new type of LCD: the LCDi. *Cornea.* 2002;21:463-468.
24. Munier FL, Frueh BE, Othenin-Girard P, et al. BIGH3 mutation spectrum in corneal dystrophies. *Invest Ophthalmol Vis Sci.* 2002;43:949-954.
25. Rozzo C, Fossarello M, Galleri G, Sole G, Serru A, Orzalesi N. A common beta ig-h3 gene mutation (delta f540) in a large cohort of Sardinian Reis Bucklers corneal dystrophy patients. Mutations in brief no. 180. *Hum Mutat.* 1998;12:215-216.
26. Fujiki K, Hotta Y, Nakayasu K, Yokoyama T, Takano T, Yamaguchi T. A new L527R mutation of the betaIGH3 gene in patients with lattice corneal dystrophy with deep stromal opacities. *Hum Genet.* 1998;103:286-289.
27. Chiti F, Stefani M, Taddei N, Ramponi G, Dobson CM. Rationalization of the effects of mutations on peptide and protein aggregation rates. *Nature.* 2003;424:805-808.
28. Xu J, Baase WA, Baldwin E, Matthews BW. The response of T4 lysozyme to large-to-small substitutions within the core and its relation to the hydrophobic effect. *Protein Sci.* 1998;7:158-177.
29. Chiti F, Taddei N, Bucciantini M, White P, Ramponi G, Dobson CM. Mutational analysis of the propensity for amyloid formation by a globular protein. *EMBO J.* 2000;19:1441-1449.
30. Fändrich M, Forge V, Buder K, Kittler M, Dobson CM, Diekmann S. Myoglobin forms amyloid fibrils by association of unfolded polypeptide segments. *Proc Natl Acad Sci USA.* 2003;100:15463-15468.
31. Morand S, Buchillier V, Maurer F, et al. Induction of apoptosis in human corneal and HeLa cells by mutated BIGH3. *Invest Ophthalmol Vis Sci.* 2003;44:2973-2979.
32. Röcken C, Stix B, Brömme D, Ansorge S, Roessner A, Böhling F. A putative role for cathepsin K in degradation of AA and AL amyloidosis. *Am J Pathol.* 2001;158:1029-1038.